Presenilin-1 influences processing of the acetylcholinesterase membrane anchor PRiMA

María-Salud García-Ayllón[1,2,3], María-Letizia Campanari[1,2], María-Fernanda Montenegro[4], Inmaculada Cuchillo-Ibáñez[1,2], Olivia Belbín[2,5], Alberto Lleó[2,5], Karl Tsim[6], Cecilio J. Vidal[4] and Javier Sáez-Valero[1,2,*]

[1]Instituto de Neurociencias de Alicante, Universidad Miguel Hernández-CSIC, Sant Joan d'Alacant, E-03550, Spain; [2]Centro de Investigación Biomédica en Red sobre Enfermedades Neurodegenerativas (CIBERNED), Spain; [3]Unidad de Investigación, Hospital General Universitario de Elche, FISABIO, Elche, Spain; [4]Departmento de Bioquímica y Biología Molecular-A, Universidad de Murcia, Spain; [5]Memory Unit, Neurology Department, Hospital de la Santa Creu i Sant Pau, Barcelona, Spain; [6]Department of Biology and Center for Chinese Medicine, The Hong Kong University of Science and Technology, Clear Water Bay Road, Hong Kong, China.

To whom correspondence should be addressed: Javier Sáez-Valero
Instituto de Neurociencias, Universidad Miguel Hernández-CSIC, E-03550 Sant Joan d'Alacant, Spain. Tel.:+34 965 91 9580, Fax:+34 965 91 9561, E-mail: j.saez@umh.es. Tel.:+34 965919580, Fax:+34 965919561.

Running title: *PS1 process AChE*

Key Words: Alzheimer's disease, γ-secretase, presenilin 1, acetylcholinesterase, PRiMA.

Number of words, Abstract: 168 w **Manuscript:** ~5600 w

Number of Figures: 7 Figures + 3 Additional Figures

Abstract

Presenilin-1 (PS1) is the catalytic component of the γ-secretase complex. In this study, we explore if PS1 participates in the processing of the cholinergic acetylcholinesterase (AChE). The major AChE variant expressed in the brain is a tetramer (G_4) bound to a proline-rich membrane anchor (PRiMA). Over-expression of the transmembrane PRiMA protein in CHO cells expressing AChE and treated with the γ-secretase inhibitor N-[N-(3,5-difluorophenacetyl)-l-alanyl]-S-phenylglycine t-butyl ester (DAPT) have enabled us to study whether, through its γ-secretase activity, PS1 participates in the processing of PRiMA-linked AChE. γ-Secretase inhibition led to a notable increase in the level of PRiMA-linked AChE, suggesting that γ-secretase is involved in the cleavage of PRiMA. We demonstrate that cleavage of PRiMA by γ-secretase results in a C-terminal PRiMA fragment. Immunofluorescence labelling allowed us to identify this PRiMA fragment in the nucleus. Moreover, we have determined changes in the proportion of the raft-residing AChE-PRiMA in a PS1conditional knockout mouse. Our results are of interest as both enzymes have therapeutic relevance for Alzheimer's disease.

1. Introduction

The accumulation of the β-amyloid peptide (Aβ) in the brain, together with the abnormal phosphorylation of the tau protein, are significant features for Alzheimer's disease (AD) pathogenesis (Blennow et al., 2006). The Aβ polypeptide arises from the proteolytic processing of a larger transmembrane protein, the amyloid precursor protein (APP), through the successive cleavage by enzymes called secretases. Sequential cleavage by β-secretase cleaving enzyme (BACE) and γ-secretase produces the Aβ peptide fragment. Alternative processing occurs if APP is first processed by a metalloproteinase, α-secretase, instead of BACE, resulting in a membrane-bound C-terminal fragment which is also a γ-secretase substrate, but generating non-amyloidogenic products (for a review see Thinakaran and Koo, 2008). γ-Secretase is a protein complex consisting of presenilin, nicastrin, APH-1 (anterior pharynx-defective 1), and PEN-2 (presenilin enhancer 2) (Kaether et al., 2006). Presenilin-1 (PS1), an aspartyl protease that cleaves substrates within the cell membrane, is the catalytic subunit of the γ-secretase complex.

Many other type-I integral membrane proteins are also known to be cleaved by γ-secretase, after a prior shedding by α-secretase or β-secretase (for a review see Lleó and Saura, 2011). We have recently demonstrated an interaction between the acetylcholine-hydrolyzing enzyme, acetylcholinesterase (AChE), and the catalytic γ-secretase component PS1 (Silveyra et al., 2008; 2012). The brain cholinergic variant of AChE (a tetramer of active subunits) is anchored to the plasma membrane through a non-catalytic subunit, a type 1 transmembrane protein called PRiMA (proline-rich membrane anchor) (Perrier et al., 2002; Chen et al., 2011). Thus, the PRiMA subunit is an accessory partner for the cellular disposition of AChE (Dobbertin et al., 1999), and represents a limiting factor for production of the tetrameric AChE (G_4)-PRiMA

complex (Perrier et al., 2003). PRiMA expression is predominantly associated to the cholinergic system and strongly co-localizes with AChE within the neurons and particularly at the plasma membrane (Henderson et al., 2010). PRiMA consists of a signal peptide, an extracellular domain that contains a proline-rich motif, a transmembrane domain, and a cytoplasmic domain (Noureddine et al., 2007). Indeed, during the progression of AD, AChE activity decreases in the cerebral cortex and other affected areas, and a major tetrameric form containing the PRiMA subunit is markedly altered, while monomeric forms of AChE are relatively preserved (Atack et al., 1983; Fishman et al., 1986; Sáez-Valero et al., 1999).

The possibility of spontaneous and evoked release of a soluble form of AChE within different brain areas has been demonstrated *in vivo* in several rodent species (Greenfield and Shaw, 1982; Appleyard and Smith, 1987; Appleyard et al., 1989), a process that is likely mediated by secretion (Anglade et al., 1999). Moreover, recently the participation of a metalloproteinase activity, likely α-secretase, has been proposed in the shedding process of plasma membrane-anchored AChE (Hicks et al., 2011; 2013). Subsequent processing of the membrane anchor subunit PRiMA, and the potential physiological consequences have been not investigated to date.

In this study we investigate whether PS1 participates in the processing of the cholinergic AChE form via cleavage of the PRiMA subunit, and whether PRiMA fragments could translocate to the nucleus. Using PS1 conditional knockout mice (PS1 cKO; Yu et al., 2001), we have also examined whether PS1 influences the localization of PRiMA-linked G_4 AChE in brain lipid rafts *in vivo*.

2. Material and methods

2.1. Cell culture and treatments

Chinese hamster ovary (CHO) cells stably over-expressing the human AChE-T variant (a generous gift from H. Soreq, The Institute of Life Sciences, The Hebrew University of Jerusalem) were cultured in DMEM+GlutaMAX™-I (Dulbecco's Modified Eagle medium; GIBCO Invitrogen Corporation) supplemented with 10% foetal bovine serum (FBS), penicillin (100 U/mL), streptomycin (100 µg/mL) and G-410 (200 µg/mL), and maintained at 37ºC in saturated humidity containing 95% air and 5% CO_2. Complete depletion of AChE from FBS was achieved by passing the seum through edrophonium-Sepharose (Flores-Flores et al., 1996). Cells were seeded at a density of 8×10^5 cells on 35 mm tissue culture dishes. CHO cells were transfected with 4 µg of PRiMA plasmid cDNA using Lipofectamine™ 2000 (Invitrogen) according to the manufacturer's instructions. The cDNA encoding the full length mouse PRiMA isoform I was tagged with an HA epitope (YPYDVP DYA) inserted before the stop codon at the C-terminus. A pCI "empty" vector (Promega, Madison, WI, USA) served as negative control. After 48 hours of the transfection, the cells were washed two times with phosphate-saline buffer (PBS) and resuspended in 120 µL ice-cold extraction buffer: 50 mM Tris-HCl, pH 7.4 / 150 mM NaCl / 5 mM EDTA / 1% (w/v) Nonidet P-40 / 0.5% (w/v) Triton X-100 supplemented with a cocktail of protease inhibitors. The cell lysates were sonicated and centrifuged at 70,000×*g* at 4 ºC for 1 hour, and the supernatants were collected and frozen at -80ºC prior to assaying for AChE and PRiMA.

CHO cells stably overexpressing wild-type human PS1 and wild-type APP (PS70, a generous gift from Dr. Selkoe; see Xia et al., 1997), were cultured in OPTIMEM supplemented with 10% FBS, and G-418 (200 µg/mL), and puromicin (2.5 µg/mL). These cells were transfected with 2 µg of PRiMA DNA and 2 µg of plasmid

DNA encoding the human AChE-T under the cytomegalovirus (CMV) promoter-enhancer (Soreq and Seidman, 2001). Cells were collected for analysis 48 hours after the transfection.

Transfected cells were treated with 0.1, 0.5, 1, 5 or 10 μM of the γ-secretase inhibitor N-[N-(3,5-difluorophenacetyl)-l-alanyl]-S-phenylglycine t-butyl ester (DAPT; Calbiochem), or vehicle (DMSO, Sigma-Aldrich Co). Alternatively, the α-secretase inhibitor Batimastat (25 μM) or the BACE inhibitor 2-β-Secretase Inhibitor III, GL189 (H-EVNstatineVAEF-NH_2; 5 μM), both from Calbiochem, Merck Chemicals, were used. Following 24 hours of treatment, cells were collected for analysis.

For some experiment, cells over-expressing AChE and PRiMA were treated for 24 hour with the neurotoxin from snake venom fasciculin-2 (Fas2; 2 nM; Abcam), which binds AChE with high affinity (Bourne et al., 2003), or with the monoclonal anti-AChE antibody HR2 (dilution 1:1000; ABR-Affinity BioReagents).

Cell viability following each treatment (as previously described) was tested in cells cultured in 96-well plates using the tetrazolium assay (MTS; CellTiter 96® AQueous Assay, Promega), according to the manufacturer's instructions.

2.2. PS1 conditional knockout mice and tissue preparation

All animal procedures were approved by the Universidad Miguel Hernandez's Animal Care and Use Committee. Brain samples were collected from ten 2.5 to 3.5 month-old PS1conditional knockout mice (*PS1* cKO; see Yu et al., 2001) and 10 age-matched littermates in a C57BL6/129 hybrid background (all generously provided by C.A. Saura, Institut de Neurociències, Universitat Autònoma de Barcelona, Spain). PS1 expression has been selectively eliminated in the postnatal forebrain of these cKO mice beginning at P18. No PS1 immunoreactivity is detected in the brains of these mice at 2–3 months

of age. In addition, no significant alterations in normal brain cytoarchitecture, neuronal number or morphology, general behaviour, motor coordination, or exploratory anxiety was observed in these mice (Yu et al., 2001; Saura et al., 2004).

Brain cortices were homogenized (10% w/v) in extraction buffer: 50 mM Tris-HCl, pH 7.4 / 500 mM NaCl / 5 mM EDTA / 1% (w/v) Nonidet P-40 / 0.5% (w/v) Triton X-100 supplemented with a cocktail of protease inhibitors (Sáez-Valero et al., 1993). The homogenates were sonicated and centrifuged as described above and the supernatants were collected and frozen at -80ºC until assay.

Raft membrane subdomains were isolated at 4ºC, as described previously but with minor modifications (Xie et al., 2010a). Briefly, brain cortices (1g/10 ml) were homogenized at 9,500 rpm (IKA, Staufen, Germany), six times (10 sec each time) in buffer A (50 mM Tris-HCl, pH 8.0, 150 mM NaCl, 5 mM benzamidine HCl, 10µg/ml aprotinin, 10µg/ml leupeptin. Homogenized tissues were then sonicated three times at low intensity (0.5 sec periods, with 30 sec intervals to avoid overheating). The sonicated preparation was centrifuged at 500 *g* for 5 min to remove cell debris and nuclei, and the post-nuclear fraction was centrifuged at 35,000 rpm for 30 min in a Sorvall TST 60.4 rotor. The resulting pellet was washed and re-suspended by sonication in 600 µl of buffer A containing 5% glycerol. This pellet was used as the total membrane fraction. For analysis of membrane rafts, a 500 µl sample of the total membrane fraction was incubated with 0.1% Triton X-100 on ice for 1 h and applied to a discontinuous flotation gradient. This fraction was then mixed with an equal volume of 80% sucrose in buffer A, placed at the bottom of a 4 mL ultracentrifugation tube, and overlaid with 2.4 mL of buffer A containing 30% sucrose followed by 0.6 ml of buffer A containing 5% sucrose. The resulting discontinuous gradient was spun at 50,000 rpm in a Sorvall TST 60.4

rotor for 18 h at 4 °C. Fourteen fractions of ~250 µl were collected from the top of the tube and used for various assays.

2.3. Nuclear protein fractionation

CHO PS70 cells were cultured in T25 flasks (8×10^5 cells/ plate). Two days after transfection with PRiMA and AChE-T, cells were washed twice with cold PBS, and gently scraped off the plates with 10 mL of cold PBS. Cell debris was discarded by centrifugation for 5 min at 500×*g*, 4ºC. Cell lysis and isolation of cellular nuclei were performed using the QProteome Nuclear Protein kit (Qiagen), according to the manufacturer's instructions. Cytosolic and nuclear protein fractions were assayed by Western Blotting using α-tubulin and acetylated histone H2B as internal markers.

2.4. Immunoprecipitation of PRiMA-HA

Immunoprecipitations were carried out at 4º C by incubating samples overnight with the antibodies coupled to protein A-sepharose using dimethyl pimelimidate dihydrochloride (Sigma-Aldrich Co). Immune complexes were eluted with glycine. For PS1 immunoprecipitation, extracts from CHO-AChE cells transfected with PRiMA were incubated with the 98/1 anti-PS1 antibody (Evin et al., 2001) and analysed by Western blotting using an anti-HA antibody. For PRiMA-HA immunoprecipitations extracts from CHO-PS1 cells transfected with PRiMA and AChE-T were incubated with the anti-HA antibody (Sigma-Aldrich Co) and analysed by Western blotting using an anti-PRiMA antibody. Extracts incubated with protein A-sepharose coupled to a non-specific rabbit IgG (Vector), were analyzed as negative controls.

2.5. AChE enzymatic assay and protein determination

A modified microassay version of the colorimetric Ellman's method was used to measure AChE (Sáez-Valero et al., 1993), using 50 μM tetraisopropyl pyrophosphoramide (*iso*-OMPA) as a specific inhibitor for the structurally related butyrylcholinesterase, an enzyme that coexists with AChE. Total protein concentrations were determined using the bicinchoninic acid method (Pierce).

2.6. Sedimentation analysis

Molecular forms of AChE were separated according to their sedimentation coefficients by centrifugation on 5-20% (w/v) sucrose gradients containing 0.5% (w/v) Triton X-100. Ultracentifugation was performed at 150,000×g in a SW 41Ti Beckman rotor for 18 hr, at 4ºC. Approximately 40 fractions were collected from the bottom of each tube and assayed for AChE activity to identify individual AChE forms (G_4 = tetramers; G_1 = monomers) by comparison with the position of molecular weight markers, catalase (11.4S) and alkaline phosphatase (6.1S). We defined the ratio of AChE forms G_4/G_1 as the proportion of G_4 molecules versus the light form, G_1.

2.7. Western blotting, measurement of PRiMA by ELISA and Phosphatase alkaline assays

Twenty to fifty micrograms of protein from cell lysates (equal amount of protein in each lane) or 40 μL of each lipid raft fraction were separated by SDS-PAGE electrophoresis. Samples were denatured at 50ºC for 15 min (PS1) or 98ºC for 7 min (all other proteins). The separated proteins were transferred to nitrocellulose membranes (Schleicher & Schuell Bioscience GmbH) and probed with the following primary antibodies: anti-AChE antibody E-19 (Santa Cruz Biotech); anti-N-terminal PS1 (Calbiochem); anti HA (Sigma-Aldrich); anti-C-terminal PRiMA (Leung et al., 1999). An anti-GAPDH

antibody (Abcam) was used as a loading control. Antibodies against flotilin 2 (BD Biosciences) was used as a lipid raft marker, whilst antibodies against calnexin (Sigma-Aldrich Co) and anti-β-cop (Thermo Scientific Pierce) were used as non-raft markers. An antibody against acetylated histone H2B (AcH2B) (generous gift of Dr. A. Barco) was used to distinguish the nuclear fraction, and an α-tubulin (Sigma-Aldrich Co) antibody was used to distinguish the cytosolic fraction. Western blots for different antibodies were performed separately to avoid re-probing of blots. The blots were incubated with the corresponding secondary antibody conjugated to horseradish peroxidase and the signal was detected using the ECL Plus detection reagent according to the manufacturer's instructions (GE Healthcare) in a Luminescent Image Analyzer LAS-1000 Plus (FUJIFILM). For semi-quantitative analysis, protein levels were normalized to GADPH and the intensity of bands was measured by densitometry with the Science Lab Image Gauge v4.0 software provided by FUJIFILM.

PRiMA levels in cortical extracts from *PS1* cKO mice were determined using specific enzyme-linked immunosorbent assays (ELISA) (Cusabio Biotech Co, Hubei, China) according to the manufacturer's instructions.

Alkaline phosphatase (AP) was measured using 0.75 mM p-nitrophenylphosphate in 0.1 mM diethanolamine buffer, pH 9.8. One unit (U) of AP activity is equal to one nmol of p-nitrophenol formed per min.

2.8. Confocal microscopy

CHO-PS1 cells were transfected with human PRiMA tagged to HA using Lipofectamine 2000 (Invitrogen) according to the manufacturer's instructions. After 4 hours, the medium was replaced with fresh medium containing 5 μM DAPT, or the equivalent volume of DMSO as vehicle control. After 24 hours, cells were washed with cold

Hank´s buffered salt solution and fixed with methanol for 10 min at -20ºC. Non-specific sites were blocked with 2% (w/v) BSA and 40 µg/mL digitonin in PBS for 30 min. Cells were then incubated with anti-HA antibody (rabbit, Sigma-Aldrich) for 1 hour followed by the secondary antibody (Cy5 anti-rabbit, GE-Healthcare) for 1 hour. After two washes with cold HBSS, cells were incubated briefly with Hoechst 33258 dye to label nuclei (Invitrogen). Pictures were acquired in a Leica upright TCL-SL confocal microscope using an HCX Plan Apochromat 63×/1.32-0.6 NA oil objective. To measure the intensity of PRiMA-HA fluorescence in the nucleus, a circle was hand drawn over the blue fluorescence of the Hoechst dye in the merge channel, and the red fluorescence from PRiMA-HA that overlapped this fluorescence was quantified. Analysis was performed with LAS AF Lite software. Non-transfected cells were used as controls, and non-specific fluorescence was not detected.

Human H4 neuroglioma cells were seeded on glass coverslips and transiently co-transfected with 300 ng of each of the AChE-T, PRiMA and PS1-GFP constructs in serum-free media using the XtremeGene9 DNA transfection reagent (Roche Diagnostics GmbH) according to the manufacturer's instructions. FBS (10%) was added to the media 4 hours after transfection. After 24 hours, the lipid rafts were labeled as described previously (Guardia-Laguarta et al., 2009). Briefly, cells on the glass coverslips were incubated with Cholera Toxin Subunit B (CT-B) tagged with an Alexa-694 fluorophore (Molecular Probes, Inc) followed by an anti-CT-B antibody (Molecular Probes, Inc) to crosslink lipid rafts into distinct patches on the plasma membrane. Cells were washed twice with PBS, fixed with 4% paraformaldehyde and then immunostained for AChE with the anti-AChE N19 antibody (Santa Cruz Biotetechnology) followed by an Alexa647-tagged secondary antibody (Molecular Probes, Inc). Confocal images were taken with a SP5 confocal microscope (Leica Microsystems GmbH, Wetzlar, Germany)

using a 63× objective (4× zoom) in three channels; 488nm (PS1-GFP), 561nm (lipid rafts) and 647nm (AChE-T). Laser power was kept at a low gain to avoid crossover between the three channels and to avoid pixel saturation. Confocal images were taken in multiple z planes (1micron apart) in order to capture the entire cell. All z planes were used for quantification of co-localization. Only the z plane at the midpoint of the cell was used for the confocal images presented here. Co-localization analysis was performed using ImageJ software (v1.46g) (Schneider et al., 2012). The three confocal channels (AChE, PS1 and lipid rafts) containing multiple z stacks across the cell were individually thresholded using the Otsu method implemented in ImageJ in order to create a binary image. Manders' coefficients (Manders, 1993) for pair-wise co-localization of either AChE-T and lipid rafts, AChE-T and PS1, or PS1 and lipid rafts were calculated for the binary threshold images using the JACoP ImageJ plug-in (Bolte and Cordelieres, 2006). The Manders' coefficients correspond to the fraction of pixels that are positive for the first protein that are also positive for the second, with a value of 1 representing 100% co-localization and 0 being 0% co-localization. Images showing the pixels where the two channels co-localize were generated for the binary threshold images using the co-localization highlighter ImageJ plug-in.

2.9. Statistical analysis

All data were analysed using SigmaStat (Version 2.0; SPSS Inc.) by Student's *t*-test (two tailed). Results are presented as means ± SEM. p values < 0.05 were considered significant.

3. Results

3.1. PRiMA interacts with PS1 and undergoes proteolytic processing

We previously demonstrated an interaction between PS1 and AChE, and the co-immunoprecipitation of G_4 AChE with PS1 antibodies (Silveyra et al., 2008). To confirm that this interaction occurs in AChE forms containing the PRiMA subunit, we used an anti-PS1 antibody to co-immunoprecipitate PRiMA in CHO cells stably over-expressing the AChE-T variant (CHO-AChE) and co-transfected with a C-terminal HA tagged PRiMA subunit. Sedimentation analysis by sucrose density gradients was used to characterize AChE molecular forms, and to confirm the expression of PRiMA-linked G_4 AChE in transfected CHO cells (Fig. 1A). Two PRiMA bands of ~22 and ~20 kDa were observed in all cellular extracts by western blot analysis with an anti-HA antibody (Fig. 1B). These two bands likely correspond to mature (fully glycosylated) and immature PRiMA (Chan et al., 2012). The specificity of the signal was confirmed in PS1 immunoprecipitates using an anti-PRiMA antibody (Fig. 1B). The PriMA signal was not detected in the negative immunoprecipitation controls, using a non-specific rabbit IgG antibody (Fig. 1C).

We next examined if γ-secretase was able to mediate PRiMA processing. CHO-AChE cells, co-transfected with PRiMA were treated with a well-known γ-secretase inhibitor DAPT, which has been demonstrated to reduce levels of Aβ in cell culture and *in vivo* (Lanz et al., 2003). The efficiency of DAPT to inhibit γ-secretase activity was monitored by measuring the accumulation of the APP C-terminal fragment (APP-CTF) in cells treated for 24 hours with 5 μM of DAPT (Fig. 2A). In cells treated with DAPT, a trend towards a decrease in soluble (secreted) AChE activity was observed, albeit that this was not statistically significant when compared to controls (12± 5%; p= 0.1). Conversely, a small but statistically significant increase (16± 6%; p= 0.03) in the

cellular AChE activity was observed compared to untreated cells (Fig. 2B). Specifically, the levels of PRiMA-linked G_4 AChE were increased in DAPT-treated cells, with minimal change in monomeric G_1 (the species devoid of PRiMA subunit), leading to a significant increase in G_4/G_1 ratio (Fig. 2C). The concomitant increase in PRiMA content (180± 40%; $p< 0.001$; Fig. 2D) in DAPT-treated cells, compared to untreated controls, suggests that PS1 can cleave PRiMA at the membrane spanning domain by preventing γ-secretase processing. A dose-dependent effect of DAPT treatment on PRiMA accumulation is observed (Supporting material, Fig. S1). No significant change in cell viability was observed following 24 hours of treatment with any of the secretase inhibitors, as assessed by the MTS method.

These results suggest that PRiMA-linked G_4 AChE is a new target of γ-secretase. However, since C-terminal fragments of PRiMA (PRiMA-CTF) were not detected in this cell line, it is possible that they were present at sub-detectable levels and is indicative of the inherent instability of these fragments. To investigate this further, CHO cell line stably transfected with PS1 (CHO PS70 cells, hereafter referred to as CHO-PS1), which exhibit elevated γ-secretase activity (Xia et al., 1997), were transfected with AChE-T and PRiMA tagged to HA at the C-terminus in an attempt to identify the PRiMA-CTF. A ~14 kDa band was detected by the anti-HA antibody corresponding to the expected size of PRiMA-CTF (Fig. 3A). The specificity of the band was confirmed by immunoprecipitation with an anti-HA antibody and Western blotting using anti-PRiMA antibody (an antibody raised to the C-terminus of PRiMA; Fig. 3B).

Moreover, accordingly with the expected sequential actions of secretases, a first one, α- or β-secretase, is expected to cleave PRiMA-linked AChE before shedding of PRiMA anchor by γ-secretase. Thus, we also monitored, under the same conditions used

for DAPT treatment, the efficiency of α- and β-secretase specific inhibitors to target PRiMA-linked AChE by determining changes in AChE release and in the cellular levels of PRiMA. Treatment of the cells with batimastat, a matrix metalloproteinase inhibitor which has previously been shown to influence AChE release (Hicks et al., 2013), prevented AChE release and increased PRiMA levels (Fig. 4). Interestingly, treatment with GL189, a specific inhibitor commonly used to block the BACE proteolytic activity of solubilized membrane fractions (Capell et al., 2002), also led to increased levels of PRiMA but the it failed to alter the levels of secreted AChE activity (Fig. 4).

We next determined whether the addition of an AChE inhibitor or an AChE antibody to the cell system, and hence associated conformational changes in the complex, would affect the processing of PRiMA. Fas2 is a strong AChE inhibitor that binds to the PAS (peripheral anionic site) rather than the active site of AChE; while HR2 is an antibody raised against human cerebellar AChE. Neither of the assayed compounds were able to induce changes in PRiMA levels (Supporting material Fig. S2), revealing that epitopes involved in these interaction are unrelated with secretase processing.

3.2. Localization of PRiMA immunoreactivity in the cell nucleus

Several transmembrane proteins have been demonstrated to undergo γ-secretase cleavage, releasing soluble intracellular fragments which translocate to the nucleus and act as transcriptional regulators (Rochette and Murphy, 2002). In contrast, other transmembrane proteins, processed by γ-secretase, are only cleaved for degradation (for a review see Lleó and Saura, 2011). Immunofluorescence labeling of nuclear DNA by DAPI allowed us to examine the presence of PRiMA-HA in the nucleus of CHO-PS1 cells transfected with PRiMA. Localization of PRiMA-HA immunoreactivity confirmed

that PRiMA-CTF enters the nucleus. The level of the nuclear PRiMA-HA signal was decreased in transfected cells treated with DAPT compared to controls (45 ±3% decrease, p= 0.002; Fig. 5A). Western blotting of HA immunoprecipitates from nuclear extracts corroborated the presence of a PRiMA-CTF in the nuclear fraction (Fig. 5B).

3.3. Co-localization of PS1 and AChE in membrane rafts

Since PS1 has been described as a lipid raft resident protein (Parkin et al., 1999; Wada 2003; Vetrivel 2004), and PRiMA can target G_4 AChE to membrane rafts (Xie et al., 2010a), we investigated whether both PS1 and PRiMA-AChE co-localize to lipid rafts. The distribution of PS1 and AChE was compared by immunocytochemistry in H4 cells (a cell line widely used for lipid raft studies; Hinz et al., 2004; Asai et al., 2007; Guardia-Laguarta et al., 2009) over-expressing both AChE-T and PRiMA subunits (Fig. 6). Confocal microscopy analysis demonstrated that ~42% of total AChE and ~10% of total PS1 co-localized with lipid rafts in H4 cells. Within the lipid rafts, ~23% of AChE co-localized with PS1 and conversely ~26% of PS1 co-localized with AChE.

3.4. The PRiMA-linked G_4 AChE form is increased in lipid rafts of the *PS1* cKO mouse brain

To assess whether γ-secretase is involved in the control of PRiMA-linked G_4 AChE levels *in vivo*, total AChE activity, AChE isoforms and PRiMA levels were measured in brain homogenates from 3-month-old *PS1* cKO mice (Yu et al., 2001) and littermate controls. No significant differences were detected in total AChE activity, PRiMA levels or in the contribution of each AChE molecular form in *PS1* cKO mice compared with littermate controls (Supporting material Fig. S3). Analyses of membrane raft preparations were then conducted in the *PS1* cKO mice to examine if PS1 influences the

localization (and/or processing) of AChE into brain lipid rafts *in vivo.* To prepare raft-enriched fractions, membrane pellets from brain cortices were treated with 0.1% Triton X-100 at 4°C and extracts subjected to flotation in discontinuous sucrose gradients. Raft-associated proteins, flotillin-2 (Volonte et al., 1999) and alkaline phosphatase (Parkin et al., 1997); and non-raft proteins, calnexin and β-cop (García-Marcos et al., 2006), were used to characterize raft enriched fractions (Fig. 7A). In the membrane preparations obtained from cortices of wild-type mice, the majority of the PS1 immunoreactivity was associated with raft membranes, whereas AChE was identified in both raft and non-raft fractions (Fig. 7B). The proportion of raft-localized AChE was higher in samples from *PS1* cKO mice than wild type mice, resulting in increased values for a quotient between raft-associated AChE and non-raft AChE, enabling the distinction between *PS1* cKO mice and littermate controls (Fig. 7C). Sedimentation analysis confirmed that the PRiMA-linked G_4 form is the major, if not the only, AChE form associated with rafts in both groups of mice (Fig. 7D).

4. Discussion

The loss of cholinergic neurons in the forebrain and the associated decline of cholinergic neurotransmission are features of AD (Davies and Maloney, 1976; Perry et al., 1977). The AChE enzyme, as part of the cholinergic system, is decreased in the brain of AD subjects, where the cholinergic PRiMA-linked G_4 form is particularly affected (Atack et al., 1983; Fishman et al., 1986). Other molecular forms and variants of AChE are present in lower quantities within the brain. These include soluble G_4 isoforms and light forms, mainly monomers, of the T ('tailed') variant (Sáez-Valero et al., 1993; 1999); and also monomers of the minor R ('readthrough') variant (Berson et al., 2003). The 3' alternative splicing of *ACHE* also generates additional N-terminally extended AChE variants (Meshorer et al., 2004). All molecular forms and variants of AChE display similar catalytic activity, however, the structural polymorphism of AChE differs within cellular compartments and between different cell types (for a review see Massoulié, 2002). It has been proposed that different molecular forms of AChE may have different physiological functions, other than its classical cholinergic role (Small et al., 1996; Grisaru et al., 1999). These polymorphisms enable the localization of AChE into particular cellular compartments. Individual components can be sorted separately by this fine regulation of AChE function (either the classical cholinergic activity or other activities), either by the protein itself or in combination with other protein partners. Recent studies have demonstrated that a significant portion of the membrane-bound G_4 AChE is localized in membrane rafts within the brain and that PRiMA directs this restricted localization (Xie et al., 2010a, 2010b). This suggests that the targeting of PRiMA-linked AChE to rafts in the brain may account for its synaptic localization and function. It is thus important to elucidate which particular AChE molecular forms are

affected in the AD brain, and within which particular cell compartment they reside, in order to optimize therapies.

In this study, we show that PS1, the catalytic component of the γ-secretase complex, can interact with the PRiMA subunit. Our data demonstrate that secretases can participate in the processing of PRiMA-linked AChE, and that PS1/γ-secretase cleaves PRiMA in a cellular model. We were also able to characterize a single 14-kDa PRiMA C-terminal fragment, and localize PRiMA immunoreactivity in the nucleus. Furthermore, the silencing of PS1 in the *PS1* cKO mouse model led to changes in the distribution of PRiMA-linked G_4 AChE forms in raft and non-raft membranes.

We have previously demonstrated that expression of the PS1-A246E pathogenic mutation in transgenic mice leads to decreased brain AChE activity (Silveyra et al., 2008). Reciprocally, AChE influences PS1 levels as AChE over-expression increases PS1 levels, while AChE knock-down with siRNA leads to decreased PS1 in transfected cells (Silveyra et al., 2011). An inter-relationship between signaling and amyloid processing has been reported for neuroligin-1, a postsynaptic adhesion molecule whose extracellular domain is homologous to AChE, and which is sequentially cleaved by α-secretase/ADAM10 and PS1/γ-secretase (Suzuki et al., 2012). This proteolytic processing of neuroligin-1 is regulated by synaptic NMDA receptor activation or interaction with soluble neurexin ligands (Suzuki et al., 2012). Whether neuronal activity regulates PS1-mediated AChE processing, and under what biological conditions, remain to be determined. It has been previously suggested that AChE shedding is related with activation of the α7 nicotinic acetylcholine receptor, and also with metabolism of APP, associated with the location of AChE into lipid raft domains (Hicks et al., 2011; 2013).

APP, one of the most investigated γ-secretase substrates, is alternatively processed through the successive actions of β-secretase and γ-secretase (amyloidogenic pathway), or by α-secretase and γ-secretase (non-amyloidogenic pathway). More than 90 type-I integral membrane proteins are known to be cleaved by γ-secretase; most of them are previously processed uniquely by α-secretase or by β-secretase, and some, similarly to APP, can be processed by both secretases (see Lleó and Saura, 2011). It is therefore important to identify the protease that cleaves PRiMA-linked G_4 prior to γ -secretase processing. Identification of these proteases will enable the design of strategies to interfere with its processing. We found that treatments with inhibitors of both, α-secretase or β-secretase, resulted in accumulation of PRiMA. Cellular treatment with batimastat, a matrix metalloproteinase inhibitor with effects in several enzymes possessing α-secretase activity, led to a significant reduction in AChE activity in the conditioned media, while, interestingly, no effect of the β-secretase inhibitor GL189 was observed. The mechanism by which AChE is released is still unclear. Our data corroborate the possibility that a metallosecretase was involved in AChE secretion (Hicks et al., 2013), while processing of PRiMA-linked AChE by β-secretase and γ-secretase may result in the degradation of the active AChE subunits. More research is needed in order to characterize difference between both pathways.

Also in this regard, it has been suggested that AChE may be targeted for endocytosis (Hu et al., 2009). Despite a large proportion of PS1 localized within the endoplasmic reticulum and early Golgi, it is assumed that APP cleavage occurs on the cell surface and in endosomes/lysosomes, where proteolytically active PS1/γ-secretase is principally localized (for a review see Haass et al., 2012). A putative domain related with endocytosis has been identified in the cytoplasmic tail of PRiMA (Hu et al., 2009). As regard with the pathological condition, this internalization pathway for AChE from

473 the cell surface to lysosomes appears to be influenced by extracellular Aβ (Hu et al.,
474 2009).

475 The identification of PS1 (Vetrivel et al., 2004), and PRiMA-linked G_4 isoforms
476 (Xie et al., 2010a, 2010b) in lipid rats, and our results showing that PS1 and PRiMA-
477 AChE interact *in vivo* (Silveyra et al., 2008) suggest that the lipid rafts maybe the
478 location of the PS1 and PRiMA-AChE interaction. Remarkably, and in accordance with
479 the subcellular sites of PRiMA-linked AChE processing by γ-secretase, while β-
480 secretase activity is enriched within lipid rafts, alongside γ-secretase (Riddell et al.,
481 2001; Hatori et al., 2006), α-secretase is not localized to rafts (Harris et al., 2009). Our
482 studies using H4 cells demonstrate that PS1 co-localizes in the same raft microdomain
483 with AChE. This is further substantiated by the observation that localization of G_4
484 AChE into rafts is altered in *PS1* cKO mice. The increased levels of raft-bound AChE in
485 the *PS1* cKO mice may arise from impaired proteolytic events resulting in decreased γ-
486 secretase activity, or from the influence of PS1 itself on the localization of AChE into
487 rafts. PS1 co-precipitates both fully glycosylated (22-kDa band) and immature PRiMA
488 (20-kDa band). PS1 has the capacity to alter both the lipid composition (Grimm et al.,
489 2006) and the lipid packing order of neuronal raft membranes (Eckert and Müller,
490 2009). Increasing evidence points to the relevance of membrane composition of both
491 raft and non-raft domains to AD progression in different AD models and in the human
492 disease (Williamson and Sutherland, 2011). The possibility that perturbations in lipid
493 rafts can influence not only APP metabolism, but also signaling events that may involve
494 cholinergic neurotransmission has been suggested (Hicks et al., 2012). Our data
495 corroborate this possibility. More interestingly, the inter-relationship between
496 neurotransmission and amyloid processing is plausible.

For the known secretase substrates, γ-secretase is always the final enzyme that cleaves the membrane-spanning domain. In general, the requirements for being a γ-secretase substrate are broad; a type I transmembrane helix with a small ectodomain (<300 amino acids), usually resulting from a prior shedding by a metalloprotease-like protease. However the requirements for γ-secretase cleavage do not depend critically on a specific amino acid sequence or on endocytosis (Struhl and Adachi, 2000). Moreover, substrates such as Notch, CD44 or the β-C-terminal fragment (β-CTF) of APP are cleaved at multiple sites by γ -secretase, resulting in various cleavage products (Lleó and Saura, 2011). In spite of the lack for specific requirements to be a potential γ-secretase substrate, it is interesting to note that the expected membrane-bound C-terminal fragment of APP and PRiMA are similar in size (~40 to 47 amino acids for the APP intracellular domain and ~40 amino acids for PRiMA). It is also worth noting that several valine residues are present at the juxtamembrane domain of PRiMA, and it is known that γ-secretase cleaves close to valines (Maruyama et al., 1996). The identification of C-terminal fragments of PRiMA is consistent with the mechanism of action of γ-secretase.

As γ-secretase cleavage of some substrates releases intracellular domains with critical signaling properties, further characterization of the generated intracellular fragment of PRiMA is required. While PRiMA intracellular fragments may be rapidly degraded, we have been able to monitor the production of a PRiMA C-terminal fragment and predict that it is translocated to the nucleus. In the absence from the PRiMA cytoplasmic tail of any of the nuclear localization signals (NLS) known to date, the possibility remains that the PRiMA fragment use an adaptor protein in its way to the nucleus. The identification of a PRiMA trans-acting cytoplasmic adaptor protein that participates and regulates the translocation will be valuable for understanding the role of

522 the PRiMA fragment in the cell nucleus. Although the occurrence of AChE in the
523 nucleus has been described in the early stages of apoptosis (Yang et al., 2002; Huang et
524 al., 2005), there is the possibility that the PRiMA segment participates in the regulation
525 of gene transcription, a possibility that deserves thoroughly investigation.

526 The physiological relevance of the proteolytic events described in this study is
527 still not well understood. AChE inhibitors are currently at the forefront of AD therapy
528 (Giacobini, 2003; Cummings, 2004; Lleó, 2007), and PS1 is a new emerging drug target
529 (Wolfe, 2008; Wagner et al., 2012). Understanding the relationship between PS1 and
530 AChE may be useful not only for the physiopathology of the disease, but also to develop
531 more effective Alzheimer therapies.

5. ACKNOWLEDGMENTS

We thank Dr. C.A. Saura (Institut de Neurociències, Departament Bioquímica i Biologia Molecular, Universitat Autònoma de Barcelona) for the *PS1* cKO mice and control littermates. We also thank Dr. H. Soreq (The Institute of Life Sciences, The Hebrew University of Jerusalem, Jerusalem, Israel) for the generous gift of the cDNA encoding T-subunit of human brain AChE and stably transfected cells, Dr. D. Selkoe (Center for Neurologic Diseases, Brigham and Women's Hospital, Boston, Massachusetts, USA) for the PS1 stably-transfected cells, Dr. J. Culvenor (Department of Pathology, The University of Melbourne, Australia) and Dr. A. Barco (Instituto de Neurociencias de Alicante, Universidad Miguel Hernández-CSIC, Spain) for generously providing antibodies. MLC is supported by a Consolider-Predoctoral fellowship from the CSIC, Spain. This work was supported by grants from Fundación CIEN-Reina Sofía, Fondo de Investigaciones Sanitarias (FIS; Grant PS09/00684) and CIBERNED, ISC-III from Spain to JSV; FIS (CP11/00067) to MSGA and PI08/0018 to AL.

In memoriam of our professor and friend Jean Massoulié.

Disclosure: None of the authors have any actual or potential financial conflicts or conflict of interest related with this study.

6. References

Anglade, P., Grassi, J., Motelica-Heino, I., Hashikawa, T., Tsuji, S., 1999. Ultrastructural evidence for dendritic release of acetylcholinesterase in the rat substantia nigra. Folia Histochem. Cytobiol. 37, 243-247.

Appleyard, M.E., Smith, A.D., 1987. Spontaneous and carbachol-evoked in vivo secretion of acetylcholinesterase from the hippocampus of the rat. Neurochem. Int. 11, 397-406.

Appleyard, M.E., Vercher, J.L., Greenfield, S.A., 1988. Release of acetylcholinesterase from the guinea-pig cerebellum in vivo. Neuroscience 25, 133-138.

Asai, M., Iwata, N., Yoshikawa, A., Aizaki, Y., Ishiura, S., Saido, T.C., Maruyama, K., 2007. Berberine alters the processing of Alzheimer's amyloid precursor protein to decrease Abeta secretion. Biochem. Biophys. Res. Commun. 352, 498-502.

Atack, J.R., Perry, E.K., Bonham, J.R., Perry, R.H., Tomlinson, B.E., Blessed, G., Fairbairn A., 1983. Molecular forms of acetylcholinesterase in senile dementia of Alzheimer type: selective loss of the intermediate (10S) form. Neurosci. Lett. 40, 199-204.

Berson, A., Knobloch, M., Hanan, M., Diamant, S., Sharoni, M., Schuppli, D., Geyer, B.C., Ravid, R., Mor, T.S., Nitsch, R.M., Soreq, H., 2008. Changes in readthrough acetylcholinesterase expression modulate amyloid-beta pathology. Brain 131, 109-119.

Blennow, K., de Leon, M.J., Zetterberg, H., 2006. Alzheimer's disease. Lancet 368, 387-403.

Bolte, S., Cordelieres, F.P., 2006. A guided tour into subcellular colocalization analysis in light microscopy. J. Microsc. 224, 213-232.

575 Bourne, Y., Taylor, P., Radic, Z., Marchot, P., 2003. Structural insights into ligand
576 interactions at the acetylcholinesterase peripheral anionic site. EMBO J. 22, 1-12.
577 Capell, A., Meyn, L., Fluhrer, R., Teplow, D.B., Walter, J., Haass, C., 2002. Apical
578 sorting of beta-secretase limits amyloid beta-peptide production. J. Biol. Chem. 277,
579 5637-5643.
580 Chan, W.K., Chen, V.P., Luk, W.K., Choi, R.C., Tsim K.W., 2012. N-linked
581 glycosylation of proline-rich membrane anchor (PRiMA) is not required for assembly
582 and trafficking of globular tetrameric acetylcholinesterase. Neurosci. Lett. 523, 71-
583 75.
584 Chen, V.P., Choi, R.C., Chan, W.K., Leung, K.W., Guo, A.J., Chan, G.K., Luk, W.K.,
585 Tsim, K.W., 2011. The assembly of proline-rich membrane anchor (PRiMA)-linked
586 acetylcholinesterase enzyme: glycosylation is required for enzymatic activity but not
587 for oligomerization. J. Biol. Chem. 286, 32948-32961.
588 Cummings, J.L., 2004. Alzheimer's disease. N. Engl. J. Med. 351, 56-67.
589 Davies, P., Maloney A.J., 1976. Selective loss of central cholinergic neurons in
590 Alzheimer's disease. Lancet 2, 1403.
591 Dobbertin, A., Hrabovska, A., Dembele, K., Camp, S., Taylor, P., Krejci, E., Bernard,
592 V., 2009. Targeting of acetylcholinesterase in neurons in vivo: a dual processing
593 function for the proline-rich membrane anchor subunit and the attachment domain on
594 the catalytic subunit. J. Neurosci. 29, 4519-4530.
595 Eckert, G.P., Müller, W.E., 2009. Presenilin 1 modifies lipid raft composition of
596 neuronal membranes. Biochem. Biophys. Res. Commun. 382, 673-677.
597 Evin, G., Sharples, R.A., Weidemann, A., Reinhard, F.B, Carbone, V., Culvenor, J.G.,
598 Holsinger, R.M., Sernee, M.F, Beyreuther, K., Masters, C.L., 2001. Aspartyl protease

599 inhibitor pepstatin binds to the presenilins of Alzheimer's disease. Biochemistry 40,
600 8359-8368.
601 Fishman, E.B., Siek, G.C., MacCallum, R.D., Bird, E.D., Volicer. L, Marquis, J.K.,
602 1986. Distribution of the molecular forms of acetylcholinesterase in human brain:
603 alterations in dementia of the Alzheimer type. Ann. Neurol. 19, 246-252.
604 Flores-Flores, C., Martinez-Martinez, A., Muñoz-Delgado, E., Vidal, C.J., 1996.
605 Conversion of acetylcholinesterase hydrophilic tetramers into amphiphilic dimers and
606 monomers. Biochem. Biophys. Res. Commun. 219, 53-58.
607 García-Marcos, M., Pochet, S., Tandel, S., Fontanils, U., Astigarraga, E., Fernández-
608 González, J.A., Kumps, A., Marino, A., Dehaye J.P., 2006. Characterization and
609 comparison of raft-like membranes isolated by two different methods from rat
610 submandibular gland cells. Biochim. Biophys. Acta. 1758, 796-806.
611 Giacobini E., 2003. Cholinergic function and Alzheimer's disease. Int. J. Geriatr.
612 Psychiatry18, S1-5.
613 Grimm, M.O., Tschäpe, J.A., Grimm, H.S, Zinser, E.G., Hartmann T., 2006. Altered
614 membrane fluidity and lipid raft composition in presenilin-deficient cells. Acta
615 Neurol. Scand. Suppl. 185, 27-32.
616 Greenfield, S.A., Shaw, S.G., 1982. Release of acetylcholinesterase and aminopeptidase
617 in vivo following infusion of amphetamine into the substantia nigra. Neuroscience 7,
618 2883-2893.
619 Grisaru, D., Sternfeld, M., Eldor, A., Glick, D., Soreq, H., 1999. Structural roles of
620 acetylcholinesterase variants in biology and pathology. Eur. J. Biochem. 264, 672-
621 686.
622 Guardia-Laguarta, C., Pera, M., Clarimón, J., Molinuevo, J.L., Sánchez-Valle, R.,
623 Lladó, A., Coma, M., Gómez-Isla, T., Blesa, R., Ferrer, I., Lleó, A., 2009. Mild

624 cholesterol depletion reduces amyloid-beta production by impairing APP trafficking
625 to the cell surface. J. Neurochem. 110, 220-230.
626 Haass, C., Kaether, C., Thinakaran, G., Sisodia, S., 2012. Trafficking and proteolytic
627 processing of APP. Cold Spring Harb. Perspect. Med. 2, a006270.
628 Harris, B., Pereira, I., Parkin, E., 2009. Targeting ADAM10 to lipid rafts in
629 neuroblastoma SH-SY5Y cells impairs amyloidogenic processing of the amyloid
630 precursor protein. Brain Res. 1296, 203-215.
631 Hattori, C., Asai, M., Onishi, H., Sasagawa, N., Hashimoto, Y., Saido, T.C., Maruyama,
632 K., Mizutani, S., Ishiura, S., 2006. BACE1 interacts with lipid raft proteins. J.
633 Neurosci. Res. 84, 912-917.
634 Henderson, Z., Matto, N., John, D., Nalivaeva, N.N., Turner, A.J., 2012. Co-localization
635 of PRiMA with acetylcholinesterase in cholinergic neurons of rat brain: an
636 immunocytochemical study. Brain Res. 1344, 34-42.
637 Hicks, D., John, D., Makova, N.Z., Henderson, Z., Nalivaeva, N.N., Turner, A.J., 2011.
638 Membrane targeting, shedding and protein interactions of brain acetylcholinesterase.
639 J. Neurochem. 116, 742-746.
640 Hicks, D.A., Nalivaeva, N.N., Turner, A.J., 2012. Lipid rafts and Alzheimer's disease:
641 protein-lipid interactions and perturbation of signaling. Front. Physiol. 3,189.
642 Hicks, D.A., Makova, N.Z., Nalivaeva, N.N., Turner, A.J., 2013. Characterisation of
643 acetylcholinesterase release from neuronal cells. Chem. Biol. Interact. 203, 302-308.
644 Hinz, B., Ramer, R., Eichele, K., Weinzierl, U., Brune K., 2004. R(+)-methanandamide-
645 induced cyclooxygenase-2 expression in H4 human neuroglioma cells: possible
646 involvement of membrane lipid rafts. Biochem. Biophys. Res. Commun. 324, 621-
647 626.

Hu, W., Gray, N.W., Brimijoin, S., 2009. Amyloid-beta alters trafficking of internalized acetylcholinesterase and dextran. Int. J. Physio.l Pathophysiol. Pharmacol. 1, 15-24.

Huang, X., Lee, B., Johnson, G., Naleway, J., Guzikowski, A., Dai, W., Darzynkiewicz, Z., 2005. Novel assay utilizing fluorochrome-tagged physostigmine (Ph-F) to in situ detect active acetylcholinesterase (AChE) induced during apoptosis. Cell Cycle 4, 140-147.

Kaether, C., Haass, C., Steiner, H., 2006. Assembly, trafficking and function of gamma-secretase. Neurodegener. Dis. 3, 275-283.

Lanz, T.A., Himes, C.S., Pallante, G., Adams, L., Yamazaki, S., Amore, B., Merchant, K.M., 2003. The gamma-secretase inhibitor N-[N-(3,5-difluorophenacetyl)-L-alanyl]-S-phenylglycine t-butyl ester reduces A beta levels in vivo in plasma and cerebrospinal fluid in young (plaque-free) and aged (plaque-bearing) Tg2576 mice. J. Pharmacol. Exp. Ther. 305, 864-871.

Leung, K.W., Xie, H.Q., Chen, V.P., Mok, M.K., Chu, G.K., Choi, R.C., Tsim, K.W., 2009. Restricted localization of proline-rich membrane anchor (PRiMA) of globular form acetylcholinesterase at the neuromuscular junctions - contribution and expression from motor neurons. FEBS J. 276, 3031-3042.

Lleó, A., Saura, C.A., 2011. γ-secretase substrates and their implications for drug development in Alzheimer's disease. Curr. Top. Med. Chem. 11,1513-1527.

Lleó, A., 2007. Current therapeutic options for Alzheimer's disease. Curr. Genomics. 8, 550-558.

Manders, E.M., Verbeek, F.J., Aten, J.A., 1993. Measurement of co-localization of objects in dual-colour confocal images. J. Microsc. 169, 375-382.

Maruyama, K., Tomita, T., Shinozaki, K., Kume, H., Asada, H., Saido, T.C., Ishiura, S., Iwatsubo, T., Obata, K., 1996. Familial Alzheimer's disease-linked mutations at

673 Val717 of amyloid precursor protein are specific for the increased secretion of A beta
674 42(43). Biochem. Biophys. Res. Commun. 227, 730-735.
675 Massoulié, J., 2002. The origin of the molecular diversity and functional anchoring of
676 cholinesterases. Neurosignals 11, 130-143.
677 Meshorer, E., Toiber, D., Zurel, D., Sahly, I., Dori, A., Cagnano, E., Schreiber, L.,
678 Grisaru, D., Tronche, F., Soreq, H., 2004. Combinatorial complexity of 5' alternative
679 acetylcholinesterase transcripts and protein products. J. Biol. Chem. 279, 29740-
680 29751.
681 Noureddine, H., Schmitt, C., Liu, W., Garbay, C., Massoulié, J., Bon, S., 2007.
682 Assembly of acetylcholinesterase tetramers by peptidic motifs from the proline-rich
683 membrane anchor, PRiMA: competition between degradation and secretion pathways
684 of heteromeric complexes. J. Biol. Chem. 282, 3487-3497.
685 Parkin, E.T., Hussain, I., Turner, A.J., Hooper, N.M., 1997. The amyloid precursor
686 protein is not enriched in caveolae-like, detergent-insoluble membrane
687 microdomains. J. Neurochem. 69, 2179-2188.
688 Parkin, E.T., Hussain, I., Karran, E.H., Turner, A.J., Hooper, N.M., 1999.
689 Characterization of detergent-insoluble complexes containing the familial
690 Alzheimer's disease-associated presenilins. J. Neurochem. 72, 1534-1543.
691 Perrier, A.L., Massoulié, J., Krejci, E., 2002. PRiMA: the membrane anchor of
692 acetylcholinesterase in the brain. Neuron 33, 275-285.
693 Perrier, N.A., Khérif, S., Perrier, A.L., Dumas, S., Mallet, J., Massoulié, J., 2003.
694 Expression of PRiMA in the mouse brain: membrane anchoring and accumulation of
695 'tailed' acetylcholinesterase. Eur. J. Neurosci. 18, 1837-1847.
696 Perry E.K., Perry R.H., Blessed G., Tomlinson B.E., 1977. Necropsy evidence of central
697 cholinergic deficits in senile dementia. Lancet 1, 189.

698 Riddell, D.R., Christie, G., Hussain, I., Dingwall, C., 2001. Compartmentalization of
699 beta-secretase (Asp2) into low-buoyant density, noncaveolar lipid rafts. Curr. Biol.
700 11, 1288-1293.
701 Rochette, M.J., Murphy, M.P., 2002. Gamma-secretase: substrates and inhibitors. Mol.
702 Neurobiol. 26, 81-95.
703 Sáez-Valero, J., Tornel, P.L., Muñoz-Delgado, E., Vidal, C.J., 1993. Amphiphilic and
704 hydrophilic forms of acetyl- and butyrylcholinesterase in human brain. J. Neurosci.
705 Res. 35, 678-689.
706 Sáez-Valero, J., Sberna, G., McLean, C.A., Small, D.H.,1999. Molecular isoform
707 distribution and glycosylation of acetylcholinesterase are altered in brain and
708 cerebrospinal fluid of patients with Alzheimer's disease. J. Neurochem. 72, 1600-
709 1608.
710 Saura, C.A., Choi, S.Y., Beglopoulos, V., Malkani, S., Zhang, D., Shankaranarayana
711 Rao, B.S., Chattarji, S., Kelleher, R.J .3rd, Kandel, E.R., Duff, K., Kirkwood, A.,
712 Shen, J. 2004. Loss of presenilin function causes impairments of memory and
713 synaptic plasticity followed by age-dependent neurodegeneration. Neuron 42, 23-36.
714 Schneider, C.A., Rasband, W.S. and Eliceiri, K.W. 2012. NIH Image to ImageJ: 25
715 years of image analysis. Nat. Methods. 9, 671-675.
716 Silveyra, M.X., Evin, G., Montenegro, M.F., Vidal, C.J., Martínez, S., Culvenor, J.G.,
717 Sáez-Valero, J. 2008. Presenilin 1 interacts with acetylcholinesterase and alters its
718 enzymatic activity and glycosylation. Mol. Cell. Biol. 28, 2908-2919.
719 Silveyra, M.X., García-Ayllón, M.S., Serra-Basante, C., Mazzoni, V., García-Gutierrez,
720 M.S., Manzanares, J., Culvenor, J.G., Sáez-Valero, J., 2012. Changes in
721 acetylcholinesterase expression are associated with altered presenilin-1 levels.
722 Neurobiol. Aging 33, 627.e27-37.

723 Small, D.H., Michaelson, S., Sberna, G., 1996. Non-classical actions of cholinesterases:
724 role in cellular differentiation, tumorigenesis and Alzheimer's disease. Neurochem.
725 Int. 28, 453-483.
726 Soreq, H., Seidman, S., 2001. Acetylcholinesterase - new roles for an old actor. Nat.
727 Rev. Neurosci. 2, 294-302.
728 Suzuki, K., Hayashi, Y., Nakahara, S., Kumazaki, H., Prox, J., Horiuchi, K., Zeng, M.,
729 Tanimura, S., Nishiyama, Y., Osawa, S., Sehara-Fujisawa, A., Saftig, P., Yokoshima,
730 S., Fukuyama, T., Matsuki, N., Koyama, R., Tomita, T., Iwatsubo, T., 2012. Activity-
731 dependent proteolytic cleavage of neuroligin-1. Neuron 76, 410-422.
732 Thinakaran, G., Koo, E.H., 2008. Amyloid precursor protein trafficking, processing, and
733 function. J. Biol. Chem. 283, 29615-29619.
734 Vetrivel, K.S., Cheng, H., Lin, W., Sakurai, T., Li, T., Nukina, N., Wong, P.C., Xu, H.,
735 Thinakaran, G., 2004. Association of gamma-secretase with lipid rafts in post-Golgi
736 and endosome membranes. J. Biol. Chem. 279, 44945-44954.
737 Volonte, D., Galbiati, F., Li, S., Nishiyama, K., Okamoto, T., Lisanti, M.P., 1999.
738 Flotillins/cavatellins are differentially expressed in cells and tissues and form a
739 hetero-oligomeric complex with caveolins in vivo. Characterization and epitope-
740 mapping of a novel flotillin-1 monoclonal antibody probe. J. Biol. Chem. 274,
741 12702-12709.
742 Wada, S., Morishima-Kawashima, M., Qi, Y., Misono, H., Shimada, Y., Ohno-Iwashita,
743 Y., Ihara, Y., 2003. Gamma-secretase activity is present in rafts but is not
744 cholesterol-dependent. Biochemistry 42, 13977-13986.
745 Wagner, S.L., Tanzi, R.E., Mobley, W.C., Galasko, D., 2012. Potential use of γ-
746 secretase modulators in the treatment of Alzheimer disease. Arch. Neurol. 69, 1255-
747 1258.

748 Williamson, R., Sutherland, C., 2011. Neuronal membranes are key to the pathogenesis
749 of Alzheimer's disease: the role of both raft and non-raft membrane domains. Curr.
750 Alzheimer Res. 8, 213-221.
751 Wolfe, M.S., 2008. Gamma-secretase inhibition and modulation for Alzheimer's
752 disease. Curr. Alzheimer Res. 5,158-164.
753 Xia, W., Zhang, J., Kholodenko, D., Citron, M., Podlisny, M.B., Teplow, D.B., Haass,
754 C., Seubert, P., Koo, E.H., Selkoe, D.J., 1997. Enhanced production and
755 oligomerization of the 42-residue amyloid beta-protein by Chinese hamster ovary
756 cells stably expressing mutant presenilins. J. Biol. Chem. 272, 7977-7982.
757 Xie, H.Q., Liang, D., Leung, K.W., Chen, V.P., Zhu, K,Y., Chan, W.K., Choi, R.C.,
758 Massoulié, J., Tsim, K.W., 2010a. Targeting acetylcholinesterase to membrane rafts:
759 a function mediated by the proline-rich membrane anchor (PRiMA) in neurons. J.
760 Biol. Chem. 285,11537-11546.
761 Xie, H.Q., Leung, K.W., Chen, V.P., Chan, G.K., Xu, S.L., Guo, A.J., Zhu, K.Y.,
762 Zheng, K.Y., Bi, C.W., Zhan, J.Y., Chan, W.K., Choi, R.C., Tsim, K.W., 2010b.
763 PRiMA directs a restricted localization of tetrameric AChE at synapses. Chem. Biol.
764 Interact. 187, 78-83.
765 Yang, L., He, H.Y., Zhang, X.J., 2002. Increased expression of intranuclear AChE
766 involved in apoptosis of SK-N-SH cells. Neurosci. Res. 42, 261-268.
767 Yu, H., Saura, C.A., Choi, S.Y., Sun, L.D., Yang, X., Handler, M., Kawarabayashi, T.,
768 Younkin, L., Fedeles, B., Wilson, M.A., Younkin, S., Kandel, E.R., Kirkwood, A.,
769 Shen, J., 2001. APP processing and synaptic plasticity in presenilin-1 conditional
770 knockout mice. Neuron 31,713-726.
771

7. Figure Legend

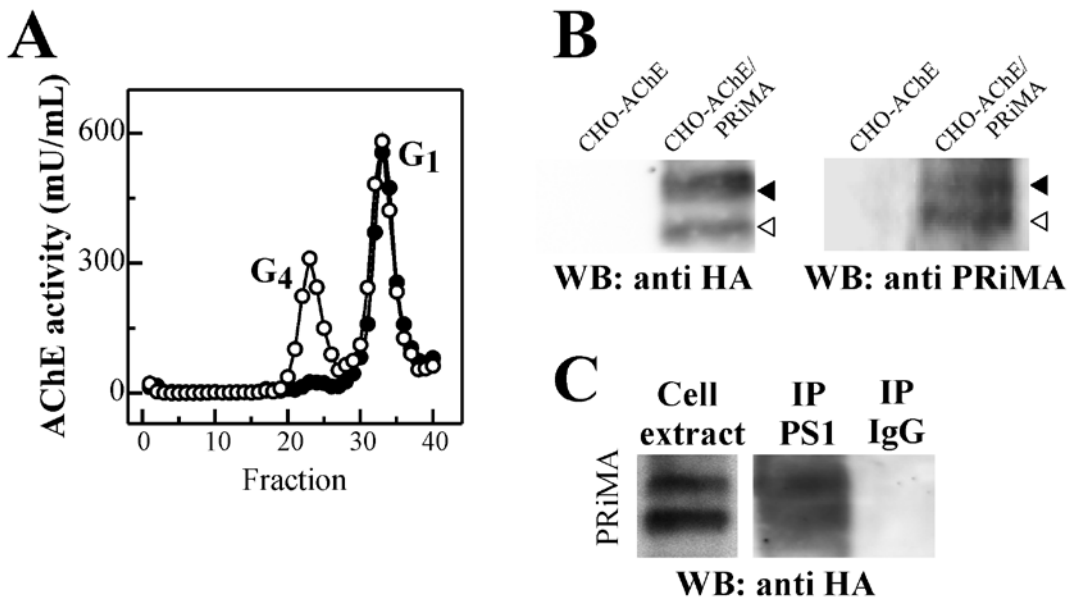

***Figure 1*. PRiMA interacts with PS1**. (**A**) Cellular extracts from CHO cells stably transfected with the AChE-T variant (CHO-AChE; open symbols) were co-transfected with the non-catalytic PRiMA subunit carrying a HA tag at its C-terminus (CHO-AChE/PRiMA; closed symbols). The generation of the tetrameric G_4 AChE form in CHO-AChE/PRiMA cells was assessed by ultracentrifugation in a continuous sucrose density gradient. (**B**) The over-expressed PRiMA subunit was identified by blotting with an anti-HA antibody or by an anti-C-terminal PRiMA antibody. Two PRiMA bands were identified at ~22 kDa (most likely the fully glycosylated mature protein; closed arrow-head) and ~20 kDa (immature protein; open arrow-head) in CHO-AChE/PRiMA cell extracts. (**C**) Cellular extracts from CHO-AChE/PRiMA cells were immunoprecipitated with an anti-N-terminal PS1 antibody. Precipitated proteins were immunoblotted with an anti-HA antibody. Two PRiMA bands at ~22 kDa and ~20 kDa were detected. Extracts incubated with protein A-Sepharose coupled with a non-specific rabbit IgG, were analyzed in parallel as negative controls.

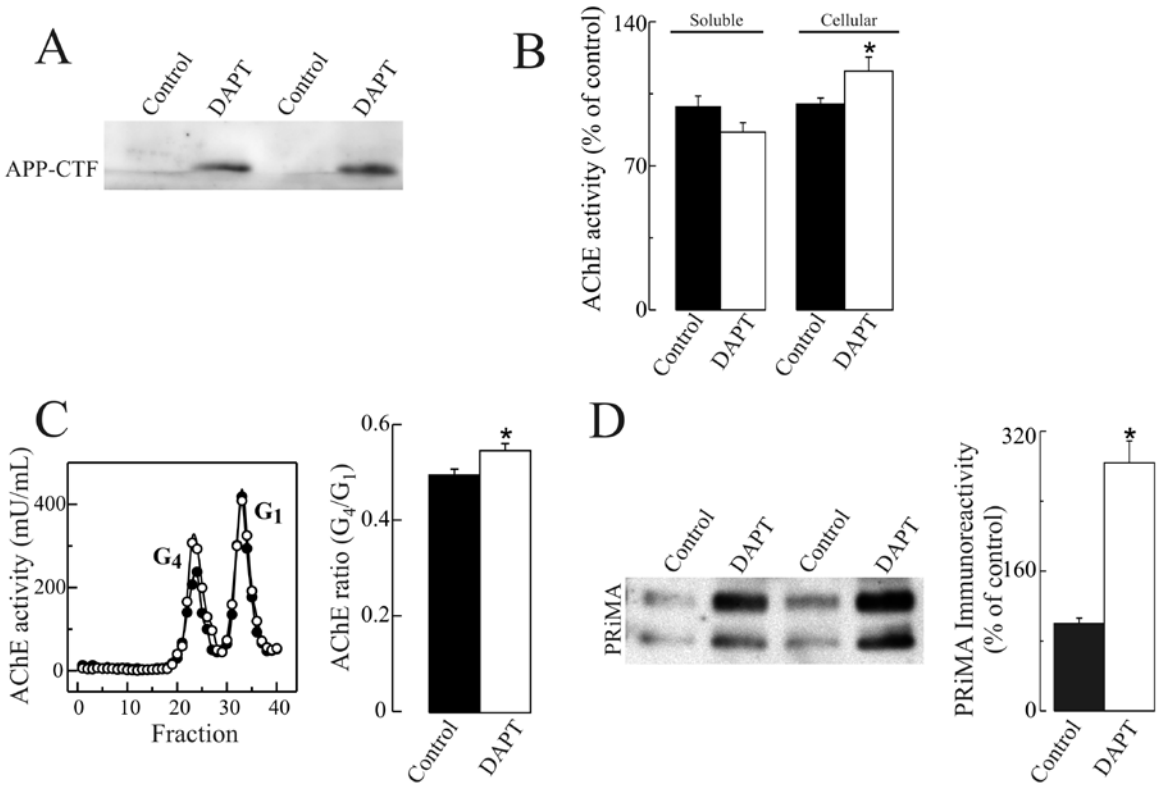

788

789 ***Figure 2*. Inhibition of γ-secretase increases levels of tetrameric AChE and of the**
790 **linked PRiMA subunit.** CHO cells stably transfected with the AChE-T variant and co-
791 transfected with PRiMA tagged to HA, were treated for 24 hours with 5 μM of DAPT or
792 vehicle control (DMSO). (**A**) The presence of the C-terminal APP fragment indicates
793 inhibition of γ-secretase activity by DAPT. (**B**) The relative percentage of soluble
794 (secreted) and cellular AChE activity after the addition of DAPT or vehicle is shown.
795 (**C**) Fractions from the sucrose density gradient were collected and assayed for AChE
796 activity to identify individual AChE isoforms in extracts from cells treated with vehicle
797 (DMSO; Control; closed symbols) or 5 μM DAPT (open symbols). The corresponding
798 G_4/G_1 ratio was calculated in controls and in DAPT treated cells. (**D**) Immunoreactivity
799 of PRiMA-HA from DAPT-treated cells. Each determination was made in duplicate.
800 Data represent means ± SEM from at least 9 independent determinations from three
801 independent experiments. *$p < 0.05$.

802

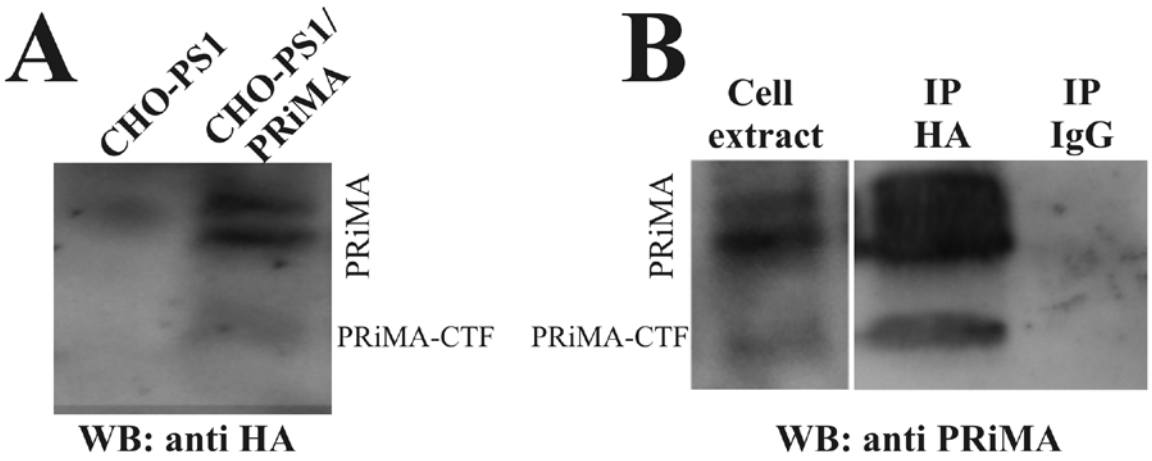

***Figure 3*. Identification of a C-terminal fragment of PRiMA in CHO-PS1 cells.** (**A**) CHO cells stably transfected with PS1 (CHO-PS1) were transfected with PRiMA tagged to HA at its C-terminus (CHO-PS1/PRiMA). The full-length PRiMA subunit and C-terminal fragment were identified by blotting with an anti-HA antibody. (**B**) Cell extracts from CHO-PS1/PRiMA cells were immunoprecipitated with an anti-HA antibody and immunoprecipitated proteins (IP) were immunoblotted with an anti C-terminal PRiMA antibody. The anti-HA antibody was able to immunoprecipitate both full length PRiMA (bands of ~22 kDa and ~20 kDa) and its CTF (~14 kDa). Negative controls were extracts incubated with protein A-sepharose coupled with rabbit IgG.

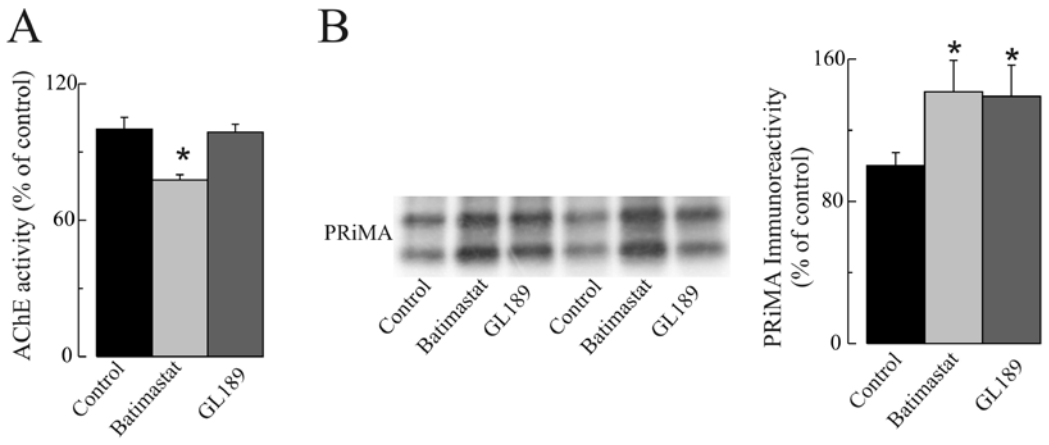

***Figure 4*. Inhibition of α-secretase and β-secretase increases levels of the PRiMA subunit.** CHO cells overexpressing AChE-T and PRiMA (tagged to HA) were treated for 24 hours with 25 μM of the α-secretase inhibitor Batimastat, with 5 μM of the β-secretase codenamed GL189, or with vehicle (control). (**A**) Soluble AChE activity was determined in conditioned media and expressed as percentage (%)with respect to control cells. (**B**) The accumulation of PRiMA was monitored with an anti-HA antibody. Data represent percentage of HA immunoreactivity relative to control cells. Data represent means ± SEM from at least 10 independent determinations from two independent experiments. *$p < 0.05$.

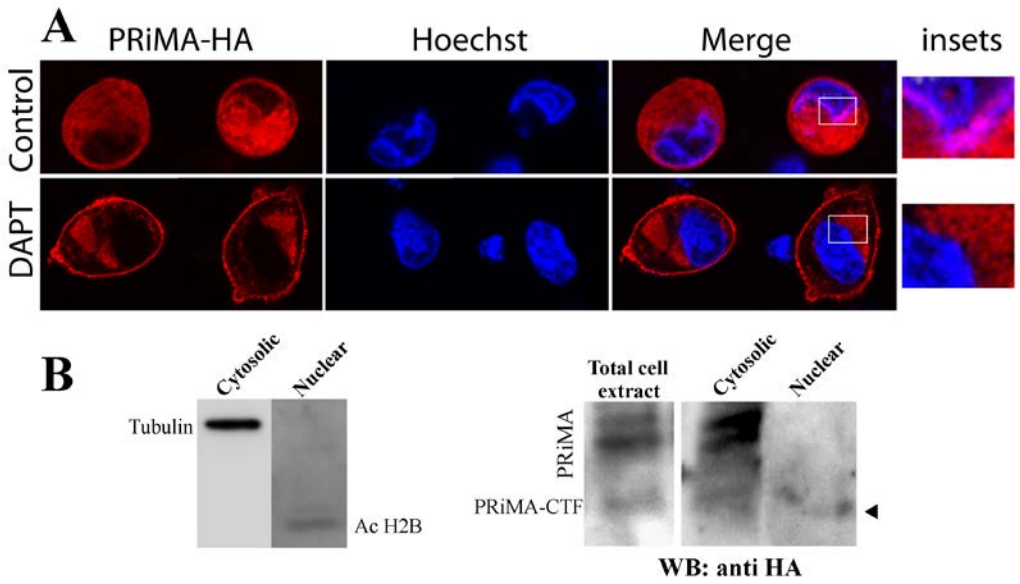

832

833 ***Figure 5*. Localization of PRiMA-HA immunoreactivity in the nucleus.** (**A**)
834 Confocal images of CHO cells stably overexpressing PS1 and co-transfected with
835 PRiMA-HA. Cells were incubated for 24 hours with DMSO (control) or with 5 µM
836 DAPT, fixed and immunodetection performed with an antibody against HA. Nuclei
837 were stained with Hoechst 33258 dye. The insets show magnification of selected areas
838 from the merged images, highlighting the low amount of PRiMA-HA in the nucleus
839 after DAPT incubation. (**B**) Nuclear and cytoplasmic fractions from CHO-PS1/PRiMA
840 cells were analyzed by Western blotting with an anti-HA antibody. A faint band of a C-
841 terminal PRiMA fragment (~14 kDa; arrow-head) was detected in the nuclear fraction
842 while full length PRiMA was detected in the cytosolic fractions. Acetylated histone
843 H2B (AcH2B) and tubulin were used as markers for nuclear and cytoplasmic fractions
844 respectively.

845

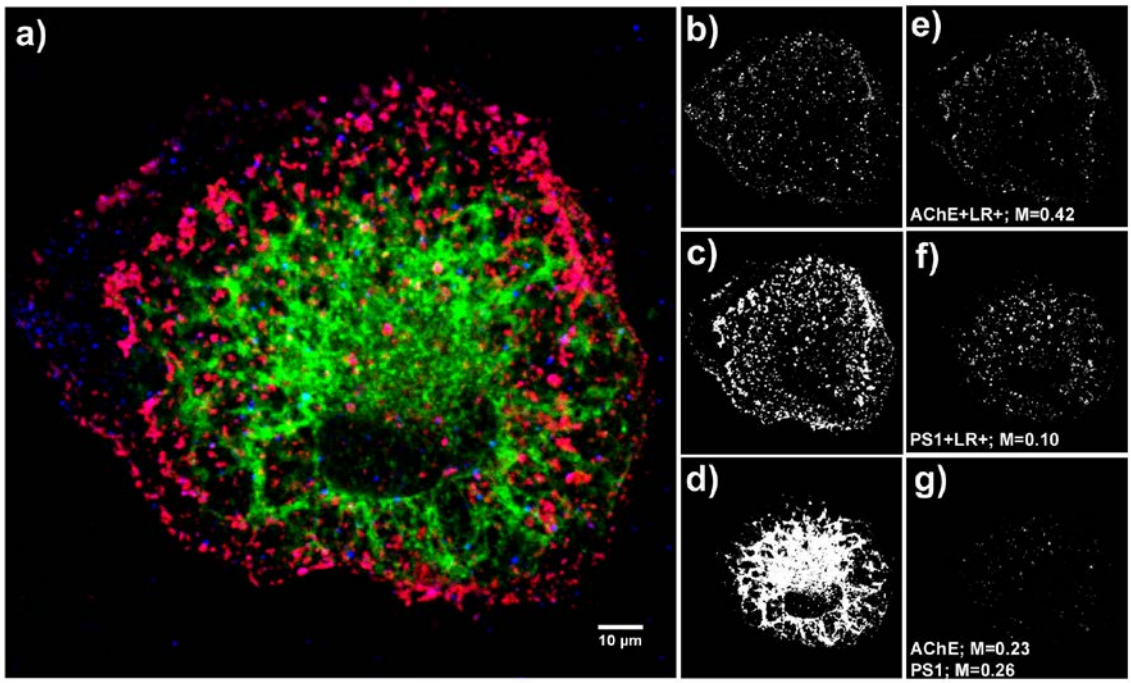

Figure 6. **AChE co-localizes with PS1 within lipid rafts. a**) H4 cell transiently expressing GFP-tagged PS1 (green), AChE (blue) and PRiMA. Lipid rafts are labelled in red. Binarised images of **b)** AChE, **c)** lipid raft and **d)** PS1 channels were generated to quantify co-localization with lipid rafts and PS1 using the Manders co-efficient (M; estimated in n= 7 cells). **e**) Pixels positive for both AChE and the lipid raft marker represent ~ 42± 3% of the total AChE-positive pixels. **f**) Pixels positive for both PS1 and the lipid raft marker represent ~10± 1% of the total PS1-positive pixels. **g**) Pixels positive for AChE, PS1 and lipid raft marker constitute approximately ~23± 5% of AChE and ~26± 4% of PS1 that localize to the lipid rafts.

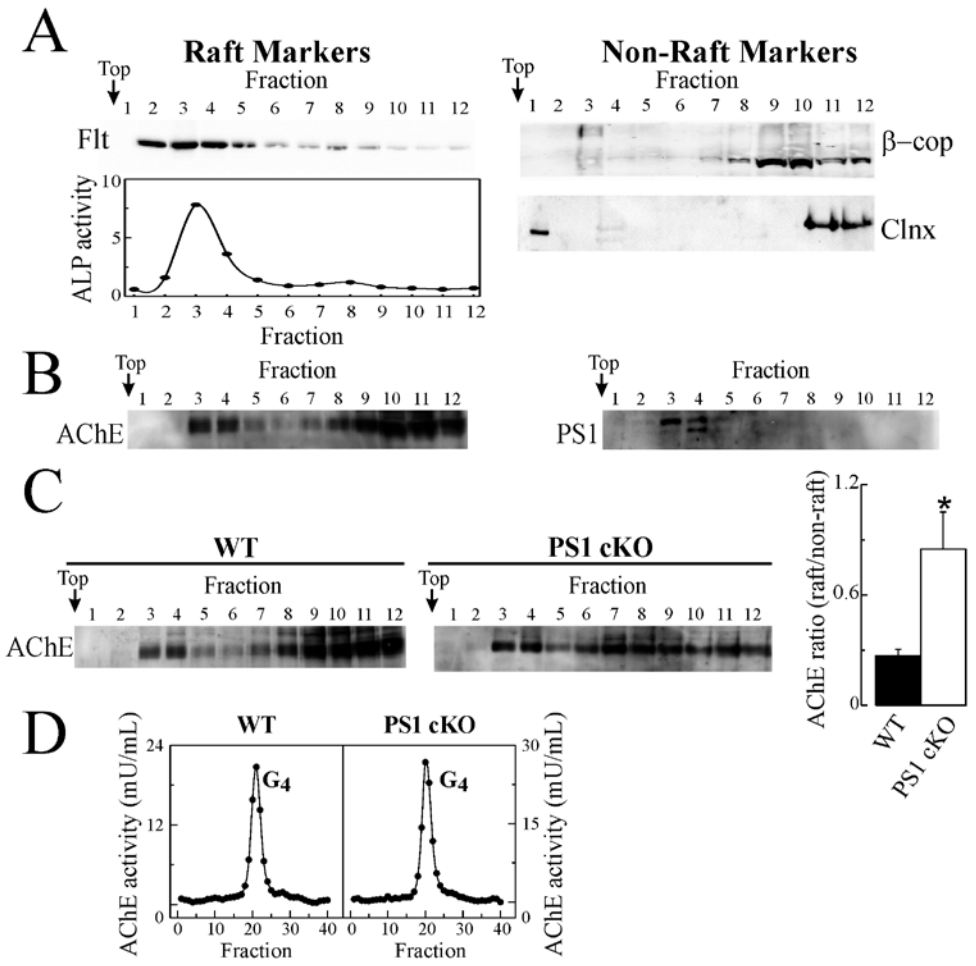

857

858 ***Figure 7.*** **G_4 AChE is increased in membrane rafts isolated from the cortex of *PS1***

859 **cKO mice.** Isolation of lipid rafts from cortices of 3-month old *PS1* cKO mice (n= 6)

860 and age-matched littermate controls (n= 6) was achieved by centrifugation in a

861 discontinuous sucrose density gradient (fractions were collected from the top of the

862 tubes). (**A**) Raft-enriched fractions (fractions 2–6) and non-raft fractions (fractions 8–

863 12) were defined after determination of positive and negative lipid raft markers. Equal

864 volumes from each fraction were analyzed by immunoblotting. Flotilin 2 (Flt) and

865 alkaline phosphatase enzymatic activity [ALP, expressed as arbitrary units (au)] were

866 used as positive lipid raft markers, and Calnexin (Clnx) and β-cop, as non-lipid raft

867 markers. (**B**) Raft localization of PS1 in control mice was verified by immunoblotting

with an anti–N-terminal PS1 antibody. Aliquots of all fractions were immunodetected with an anti–N-terminal antibody E19, which recognizes all the variant subunits of AChE. AChE and PS1 were localized in lipid raft rich fractions as determined in (**A**). (**C**) Immunoblotting demonstrated increased AChE partitioning into lipid raft fractions in *PS1* cKO versus control mice, as assessed by a ratio of the densitometric quantitation of the immunoreactivity of AChE bands identified in raft fractions 2–6 divided by the immunoreactivity of AChE bands identified in non-raft fractions 8–12. (**D**) Sedimentation analysis of raft-residing AChE (fractions 2-6) demonstrated a single molecular form corresponding to PRiMA-linked G_4 AChE in both WT and *PS1* cKO mice.

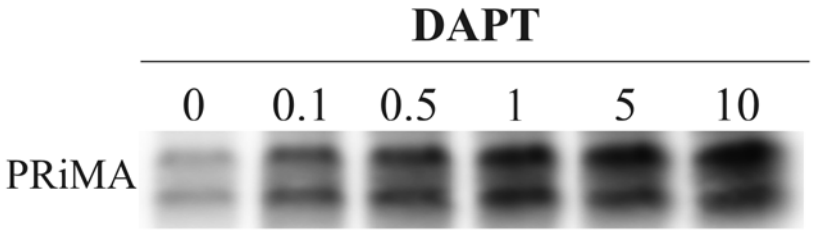

878
879 ***Additional Figure 1*. Dose-dependent effect of the γ-secretase inhibitor DAPT on**
880 **PRiMA processing.** CHO cells stably transfected with the AChE-T variant and co-
881 transfected with the PRiMA subunit tagged to HA were treated with 0 (no treatment
882 control), 0.1, 0.5, 1, 5 or 10 μM of DAPT. Cellular extracts immunoblotted with an anti-
883 HA antibody demonstrated increased PRiMA levels in treated cells. The results were
884 confirmed in three independent experiments.
885

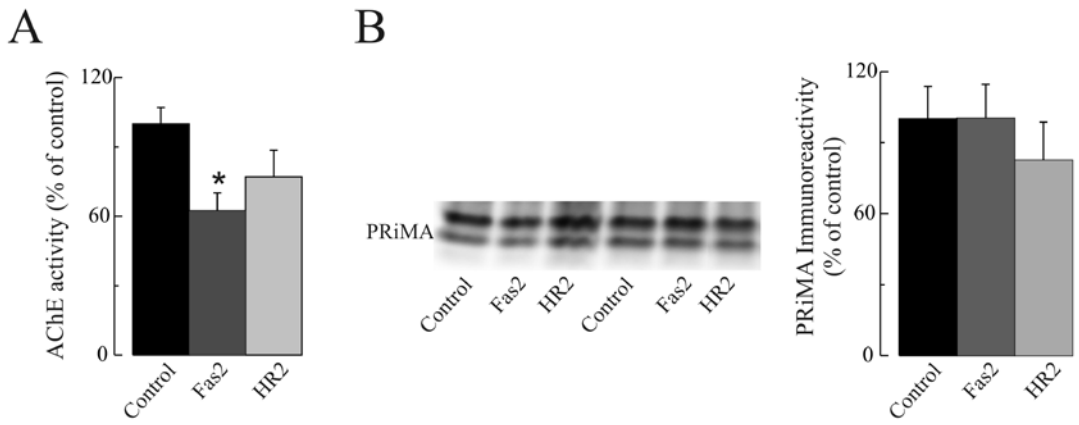

886

887 ***Additional Figure 2*. Unaltered levels of PRiMA in cells incubated with the AChE**
888 **inhibitor fasciculin-2 and with the anti-AChE antibody HR2.** CHO cells stably
889 transfected with the AChE-T variant and co-transfected with PRiMA tagged to HA,
890 were treated for 24 hours with fasciculin-2 (Fas2; 2 nM), or with the antibody HR2
891 (dilution 1:1000). **(A**) The relative percentage of soluble AChE activity present in
892 conditioned media after the addition of the specific reagent is shown. (**B**)
893 Immunoreactivity of PRiMA-HA from treated cells. Each determination was made in
894 duplicate. Data represent means ± SEM from at least 10 independent determinations
895 from two independent experiments. *$p < 0.05$.

896

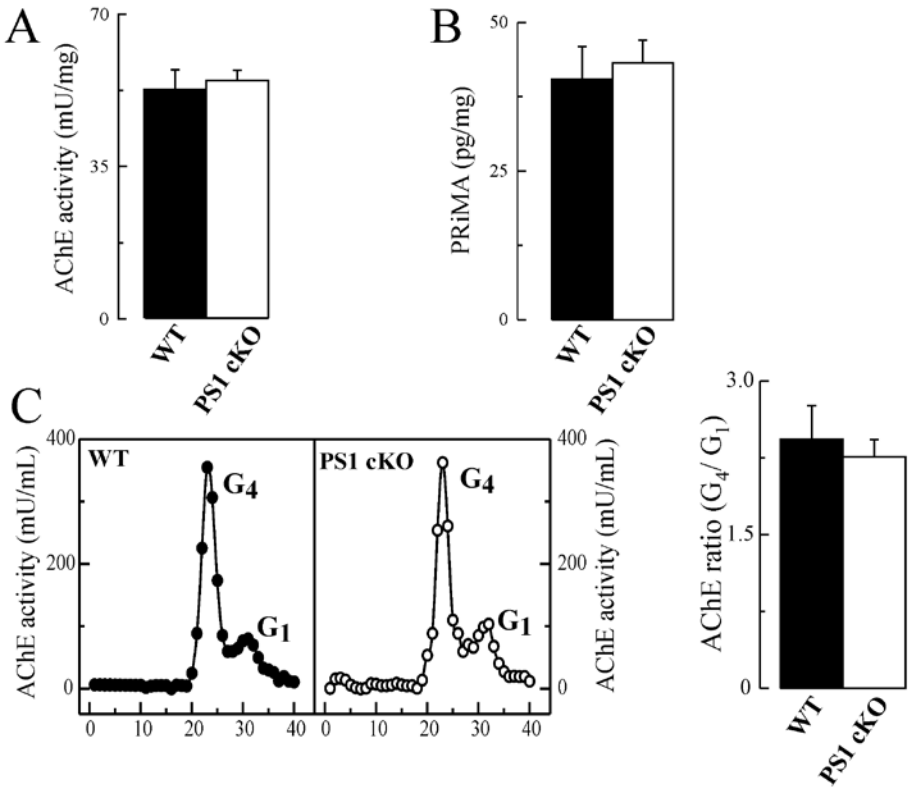

897

898 ***Additional Figure 3*. Levels of AChE remain unchanged in the *PS1* cKO mouse**
899 **brain.** (**A**) Levels of AChE specific activity and (**B**) of PRiMA (assessed by a
900 commercially available ELISA kit for mouse PRiMA) were measured in cortical
901 extracts from 3-month old *PS1* cKO mice (n= 6) and age-matched littermate controls
902 (wild type: WT; n= 6). No difference in activity (AChE) or levels (PRiMA) was
903 observed between WT and *PS1* cKO mice. (**C**) Representative profiles and levels of
904 molecular AChE forms in cortical extracts are also presented. The major AChE
905 component corresponds to amphiphilic tetramers (G_4), with minor amounts of
906 monomeric forms (G_1). No significant difference in levels was observed between WT
907 and *PS1* cKO mice.